# Visual specialization of an herbivore prey species, the white-tailed deer

**G.J. D'Angelo, A. Glasser, M. Wendt, G.A. Williams, D.A. Osborn, G.R. Gallagher, R.J. Warren, K.V. Miller, and M.T. Pardue**

**Abstract:** To gain knowledge of visual specializations influencing the behavior of white-tailed deer (*Odocoileus virginianus* (Zimmermann, 1780)), we examined gross eye characteristics, structural organization of the retina, and the density and distribution of cone photoreceptors. White-tailed deer possess ocular features similar to other ungulates including a horizontal slit pupil, reflective tapetum lucidum, typical retinal structure, and medium wavelength sensitive cone photoreceptors concentrated in a horizontal visual streak. The tapetum was found to cover the superior portion of the eye and overlapped the horizontal visual streak. Comparisons between fawns and adults did not reveal any differences in retinal thickness, retinal nuclei counts, or cone photoreceptor counts. While M-cones had increased density in the visual streak, S-cones were distributed evenly across the entire retina. Schematic eye calculations of a 0.5-year-old deer indicated a hyperopic eye (+7.96) with a F/# ranging from 5.55 to 1.39 for pupil diameters of 3 to 12 mm. As expected for a crepuscularly active prey species, the visual system of white-tailed deer is specialized for sensitivity in low-light conditions and detection of predators.

**Résumé :** Afin de connaître les spécialisations visuelles qui influencent le comportement du cerf de Virginie (*Odocoileus virginianus* (Zimmermann, 1780)), nous avons examiné les caractéristiques grossières de l'œil et l'organisation structurale de la rétine et déterminé la densité et la répartition des cônes photorécepteurs. Les cerfs de Virginie possèdent des caractéristiques oculaires semblables à celles d'autres ongulés, en particulier une pupille à fente horizontale, un tapetum lucidum réfléchissant, une structure rétinienne typique et des cônes photorécepteurs sensibles aux longueurs d'onde moyennes concentrés dans une bande visuelle horizontale. Le tapetum couvre la portion supérieure de l'oeil et recouvre la bande visuelle horizontale. Des comparaisons entre les faons et les adultes ne montrent aucune différence dans l'épaisseur de la rétine, le dénombrement des noyaux rétiniens, ni le dénombrement de cônes photorécepteurs. Alors que les cônes M ont une densité plus élevée dans la bande visuelle, les cônes S se répartissent uniformément sur toute la rétine. Des calculs schématiques de l'œil d'un cerf âgé de 0,5 an indiquent que l'œil est hypermétrope (+7,96) avec une valeur de F/# variant de 5,55 à 1,39 pour des diamètres de pupille de 3 à 12 mm. Comme on peut s'y attendre chez une espèce active au crépuscule, le système visuel du cerf de Virginie se spécialise pour une sensibilité aux conditions de lumière basses et pour la détection des prédateurs.

[Traduit par la Rédaction]

## Introduction

White-tailed deer (*Odocoileus virginianus* (Zimmermann, 1780)) are widely extant from the tropics to the arctic in a variety of habitats ranging from densely vegetated coastal wetlands to open prairies (Geist 1998). Their circadian activity patterns are typically described as arrhythmic with peaks in activity near dawn and dusk (Marchinton and Hirth 1984). In diverse habitats and lighting conditions, white-tailed deer must rely on vision for avoidance of predators, foraging, intraspecific communication, and general negotiation of their home ranges. Although many aspects of their biology have been studied thoroughly, the visual abilities of white-tailed deer continue to be the subject of much discussion and conjecture within the scientific and deer-hunting communities. Knowledge of deer vision may provide a foundation toward understanding deer behavior and antipredation strategies, and may be useful for developing physiologically based strategies to reduce deer–human conflicts.

White-tailed deer have a typical mammalian eye (Walls 1942). Light enters the eye through the cornea, passes through the aqueous humor, the pupil, the lens, and the vit-

Received 8 June 2007. Accepted 7 April 2008. Published on the NRC Research Press Web site at cjz.nrc.ca on 24 June 2008.

**G.J. D'Angelo,[1,2] D.A. Osborn, R.J. Warren, and K.V. Miller.** Daniel B. Warnell School of Forestry and Natural Resources, University of Georgia, Athens, GA 30602, USA.
**A. Glasser and M. Wendt.** School of Optometry, University of Houston, Houston, TX 77204, USA.
**G.A. Williams.** Neuroscience Research Institute and Department of Psychology, University of California, Santa Barbara, CA 93106, USA.
**G.R. Gallagher.** Department of Animal Sciences, Berry College, Mount Berry, GA 30149, USA.
**M.T. Pardue.** Research Service, Atlanta VA Medical Center, Decatur, GA 30033, USA; Department of Ophthalmology, Emory University, Atlanta, GA 30033, USA.

[1]Corresponding author (e-mail: Gino.J.DAngelo@aphis.usda.gov).
[2]Present address: US Department of Agriculture – Animal and Plant Health Inspection Service (USDA–APHIS) Wildlife Services, 3092 Sugan Road, Solebury, PA 18963, USA.

 doi:10.1139/Z08-050 

reous body before striking the retina, a layered neural structure at the back of the eye. The cornea is the first optical element to refract light. The pupil restricts the amount of light entering the rest of the eye. The optics of the cornea and lens invert and focus the image on the retina (Ali and Klyne 1985). The retina is the brain's visual pathway and is organized in layers of interconnected cells, the most prominent of which are the rod and cone photoreceptors. Photoreceptors are highly specialized neurons which contain light-sensitive photopigment molecules that absorb light. The rod photoreceptors are responsible for vision in low-light conditions, whereas the cone photoreceptors provide the basis for color vision and distinguish fine detail.

Witzel et al. (1978) confirmed the presence of rods and cones in the white-tailed deer retina. They found cones at densities of about 10 000/mm$^2$ in the central retina; however, their examination did not include systematic surveys across the entire retina or classification of different types of cones. With electroretinogram flicker photometry, Jacobs et al. (1994) detected the presence of two classes of cone photopigments in white-tailed deer, one maximally sensitive to medium wavelengths ($\lambda_{max}$ = 537 nm) and the other with peak sensitivity to short wavelengths ($\lambda_{max}$ = 450–460 nm), in addition to rod photoreceptors ($\lambda_{max}$ = 497 nm). Staknis and Simmons (1990) failed to identify the presence of cones, but rods were readily visible at all locations they sampled with scanning and transmission electron microscopy. The discrepancies among the aforementioned studies suggest that cones may not be evenly distributed throughout the retina of white-tailed deer.

Based on data from other ungulates, Müller-Schwarze (1994) speculated that all species of deer have a visual streak corresponding to a horizontal band of increased cellular density in the retina, which affords them increased acuity. Recently, Ahnelt et al. (2006) found that two species of cervids, red deer (*Cervus elaphus* L., 1758; also known as wapiti or elk) and western roe deer (*Capreolus capreolus* (L., 1758)), have an arrangement of medium-wavelength cones characteristic of a horizontal visual streak. No data exist on the density and distribution of cones throughout the white-tailed deer retina. Our objectives were (*i*) to describe the gross morphology of the white-tailed deer eye integral to understanding retinal function, (*ii*) to examine the microscopic structure of the white-tailed deer retina, (*iii*) to determine the density and distribution of cones in the white-tailed deer retina to identify whether they possess a visual streak.

## Materials and methods

### Study area and animals

White-tailed deer were collected on the Daniel B. Warnell School of Forestry and Natural Resources Whitehall Experimental Forest (WEF), a 337 ha property on the campus of the University of Georgia, Athens, Georgia. WEF was located in the Piedmont Uplands physiographic province, and was bordered on three sides by the Oconee River. From 22 to 28 November 2006, eyes from six free-ranging female white-tailed deer were obtained, including three fawns (~0.5 years old) and three adults (2.5 years old, $n$ = 1; 3.5 years old, $n$ = 1; 6.5 years old, $n$ = 1). All deer included in our sample appeared healthy with no signs of ocular disease.

### Dissection and gross measurements

All animal procedures were performed following the *Canadian Journal of Zoology* guidelines, with prior approval from the University of Georgia Institutional Animal Care and Use Committee (no. A2004-10102-0), and under the authorization of a Georgia Department of Natural Resources Wildlife Resources Division scientific collection permit (no. 29-WSF-05-115).

Free-ranging white-tailed deer were euthanized by sharpshooting with a high-powered rifle. Gross eye measurements were made with digital vernier calipers (Mitutoyo Corporation, Kawasaki, Japan) accurate to ±0.2 mm. Immediately after death, interocular distance was measured, a dorsal orientation mark was created in the cornea with a heated dissecting needle, and the eyes were enucleated. The external gross eye measurements included axial length (anterior corneal surface to posterior sclera adjacent to optic nerve), vertical and horizontal equatorial diameters (greatest diameter of whole intact eye), and vertical and horizontal corneal diameters (measured from limbus margins).

One eye of each deer was used for gross external measurements and then dissected to obtain measurements of corneal thickness (central and peripheral), as well as lens diameter and thickness. The remaining eyecups were fixed in 4% paraformaldehyde for 24 h. The retina was then dissected from the eyecup and the tapetum lucidum, and radial incisions were made to flatten the retina in preparation for subsequent mounting on slides. Following processing of the eyes, the age of the deer was estimated by tooth wear and replacement criteria (Severinghaus 1949).

### Histology

For the opposite eye of each deer, gross external measurements were made and then a solution of 2% paraformaldehyde/2.5% glutaraldehyde was injected into the anterior and vitreous chambers with a syringe and small gauge needle. The whole eye was immersed in a solution of 2% paraformaldehyde/2.5% glutaraldehyde for >24 h. Subsequently, each eye was equatorially bisected and photographed. The temporal half was further dissected and processed into epoxy resin while the nasal half was embedded whole in paraffin for further sectioning. Orientation of all tissue samples were noted throughout processing.

To measure retinal layer thickness, retinal tissue samples were taken superior and inferior to the optic nerve. Tissue samples were dehydrated through a graded series of alcohols, embedded in plastic (Embed 812-Der 736; Electron Microscopy Sciences, Hartfield, Pennsylvania), and serially sectioned (thickness = 0.5 μm) on an ultramicrotome (Reichert Ultracut; Leica, Bannockburn, Illinois) using a diamond knife. All retinal tissue sections were stained with toluidine blue.

Paraffin sections of the whole eye were found to have distortions that prevented measurement of retinal layer thickness. These sections will be used for a future study examining the anterior segment of the deer eye.

Using a light microscope (Leica DMLB Microscopy, Ban-

nockburn, Illinois) and CCD camera (Leica DC 300F, Bannockburn, Illinois) retinal sections were photographed. Micrographs were imported into Image-Pro Plus software (Media Cybernetics, Bethesda, Maryland) and the thickness of the total retina, as well as each individual retinal layer, was measured. In addition, a single area superior to the optic nerve, approximately in the visual streak and 110 μm in length, was used for counts of ganglion cell layer nuclei, inner nuclear layer nuclei, and rows of photoreceptor nuclei.

### Immunohistochemistry

All immunohistochemical steps were performed at 4 °C on a rotator. Retinas were immersed in phosphate-buffered saline (PBS) for three 5 min rinses followed by a 1 h rinse. Retinas were immersed for 12 h in 10% normal goat serum (1:20; Jackson ImmunoResearch Laboratories, Inc., West Grove, Pennsylvania) diluted in a solution of PBS, 0.5% bovine serum albumin (Sigma, St. Louis, Missouri), Triton X-100 (LabChem Inc., Pittsburgh, Pennsylvania), and 0.1% sodium azide (Sigma, St. Louis, Missouri; PBTA). Primary antibodies diluted in PBTA were applied to retinas for 72 h. Primary antibodies consisted of either antisera JH455 (1:5000 dilution) to label the short-wavelength cone opsin (S-antibody-labeled cones) or antisera JH492 (1:5000 dilution) to label the medium-wavelength cone opsin (M-antibody-labeled cones); both antibodies were gifts of Dr. Jeremy Nathans. Following incubation in the primary antibody, retinas were again rinsed in PBTA, followed by incubation in goat anti-rabbit IgG secondary antibody conjugated to the fluorophore Rhodamine (Tetramethyl Rhodamine Isothiocyanate; Jackson ImmunoResearch Laboratories, West Grove, Pennsylvania) diluted in PBTA for 24 h. Before mounting, retinas were rinsed and then flat-mounted in mounting medium (Vector Laboratories, Inc., Burlingame, California). A cover slip was applied and sealed with nail polish. Shrinkage of retinal tissue was considered to be negligible.

To count immunoreactive cones, 1 mm intervals were surveyed across the retina in 0.0024 $mm^2$ sampling windows using a fluorescent light microscope (Nikon, Melville, New York) and a CCD camera (Princeton Scientific Instruments, Inc., Monmouth Junction, New Jersey). On average, 1179 locations were sampled in each retina examined. Distribution maps were developed for densities of S-antibody-labeled cones and M-antibody-labeled cones of individual retinas.

### Data analysis

Mean gross eye measurements were calculated for fawns (0.5 years old) and adults (>1.0 years old). We calculated lens thickness ratio by dividing lens thickness by axial length. Gross eye measurements were compared between fawns and adults with a Student's *t* test.

The mean thickness measurement was averaged for the two retinal locations and a comparison made between fawns and adults using Student's *t* test. Similar analyses were made for the cell counts of each nuclear layer.

To obtain the mean photoreceptor density per square millimetre of cones reactive for each of the two cone-opsin-specific antibodies for each retina in immunohistochemical experiments, labeled cone densities were averaged across all retinal locations. Cone densitiesper square millimetre were then averaged for all retinas labeled with either S- or M-cone-opsin-specific antibodies.

**Fig. 1.** Enucleated eye of white-tailed deer (*Odocoileus virginianus*: 1, cornea; 2, lens; 3, ciliary body; 4, retina; 5, optic nerve head. The eye was dissected bilaterally and photographed in four parts at 0.8× magnification. In Adobe Photoshop CS3 (San Jose, California), the photographs of the four parts were merged with no further alterations to the images. Readers should note that the eye was fixed in a solution of 2% paraformaldehyde/2.5% glutaraldehyde, which altered the coloration and opacity of the eye. The white bands outlining the cornea, lens, and sclera are reflections from the light source.

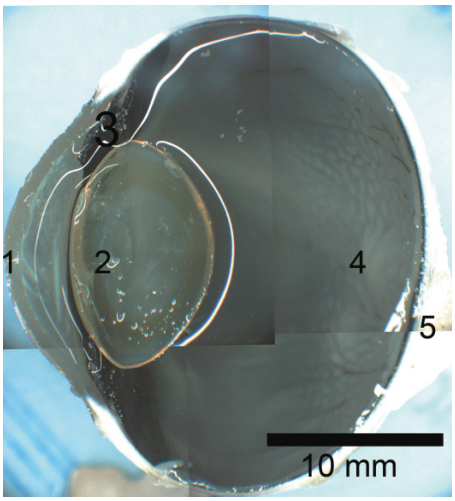


### Schematic eye

Surface curvature data (anterior corneal curvature, posterior corneal curvature, anterior lens curvature, and posterior lens curvature) and axial distance measurements (corneal thickness, anterior chamber depth, lens thickness, and vitreous chamber depth) were measured from the cross-section of the fixed deer eye shown in Fig. 1 using MATLAB image analysis software. The curvature data were approximated as spherical surfaces. Each measurement was made five times and then averaged for a mean value of that structure. A schematic eye was constructed from these values using an optical ray tracing program (ZEMAX; Zemax, Bellevue, Washington). To generate the f-number (F/#), the effective focal length of the eye divided by the entrance pupil diameter, the schematic eye was modeled to have parallel light entering the eye from the left. The schematic eye was then "refracted" with an infinitely thin trial lens placed at the corneal vertex optimized to provide the trial lens focal length necessary to achieve a minimum image spot size on the retina. The F/# was generated by ZEMAX using a range of entrance pupil diameters (3, 6, 9, and 12 mm). The sensitivity of the F/# to the refractive error of the model eye was tested by optimizing the schematic eye to emmetropia by adjusting the vitreous chamber depth to minimize the image spot size on the retina.

## Results

The white-tailed deer eyes were approximately spherical based on equatorial and axial measurements (Table 1,

**Table 1.** Measurements of anatomical features of eyes of white-tailed deer (*Odocoileus virginianus*).

| | Fawns | | Adults | | | | |
|---|---|---|---|---|---|---|---|
| | Mean | SE | Mean | SE | *t* | df | *P* |
| Interocular distance (mm) | 81.1 | 0.2 | 94.9 | 1.9 | –3.521 | 4 | 0.012 |
| Axial length (mm) | 25.3 | 0.2 | 27.8 | 0.2 | –7.082 | 10 | <0.0001 |
| Vertical equatorial diameter (mm) | 26.5 | 0.2 | 28.7 | 0.2 | –5.420 | 10 | 0.0001 |
| Horizontal equatorial diameter (mm) | 27.0 | 0.2 | 28.6 | 0.2 | –4.159 | 10 | 0.0009 |
| Vertical corneal diameter (mm) | 17.7 | 0.2 | 19.7 | 0.3 | –3.729 | 10 | 0.002 |
| Horizontal corneal diameter (mm) | 19.9 | 0.2 | 22.0 | 0.2 | –4.491 | 10 | 0.0006 |
| Central corneal thickness (mm) | 0.6 | 0.1 | 0.6 | 0.1 | 0.417 | 4 | 0.349 |
| Peripheral corneal thickness (mm) | 0.5 | 0.1 | 0.5 | 0.0 | –0.277 | 4 | 0.398 |
| Vertical pupil diameter (mm) | 12.8 | 0.3 | 15.4 | 0.3 | –4.307 | 10 | 0.0008 |
| Horizontal pupil diameter (mm) | 14.2 | 0.1 | 15.6 | 0.3 | –2.908 | 10 | 0.008 |
| Lens diameter (mm) | 13.0 | 0.1 | 14.3 | 0.3 | –2.697 | 4 | 0.027 |
| Lens thickness (mm) | 7.4 | 0.2 | 9.2 | 0.4 | –2.659 | 4 | 0.028 |

**Note:** Fawns ($n$ = 3) were 0.5 years old and adults ($n$ = 3) ranged from 2.5 to 6.5 years old.

**Fig. 2.** Radially flattened ocular fundus of white-tailed deer (*Odocoileus virginianus*). The eye was fixed in 4% paraformaldehyde, which slightly altered the coloration of the ocular fundus. The white circle indicates the location of the optic nerve head with the medium gray, light gray (or blue, blue–green on the Web version) tapetum located superior to the optic nerve.

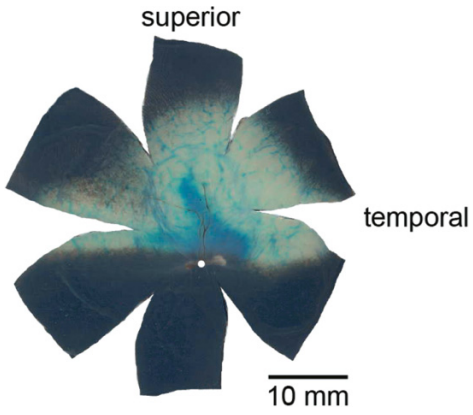


Fig. 1). The corneas were oval as viewed along the optical axis, with the length of the horizontal corneal diameter exceeding the length of the vertical corneal diameter ($t_{[22]}$ = –4.20, $P$ = 0.0002, $n$ = 12). With the exception of central and peripheral corneal thicknesses, all gross measurements of the eyes of adult deer exceeded those of fawns (Table 1). However, lens thickness to axial length ratio did not differ among fawns and adults (pooled mean = 0.3, SE = 0.01, $t_{[4]}$ = –1.76, $P$ = 0.08, $n$ = 6). The pupil was a horizontal slit.

The tapetum lucidum was a prominent half moon shape radiating from a point on the inferior border centered approximately 1 mm superior to the optic nerve head, and extending about two-thirds into the superior retina (Fig. 2). The tapetum covered a greater portion of the superior, temporal retina. The inferior border of the tapetum was nearly horizontal. The tapetum was iridescent, and reflected an azure blue color centrally, transitioning to blue–green and yellow in its periphery (colours visible on the Web version of Fig. 2).

The retina had typical vertebrate structure with all the retinal layers present (Fig. 3). All retinas showed some signs of edema, likely owed to a delay in fixation. The retinal layer thickness measurements are shown in Table 2. No differences were found between the areas inferior and superior to the optic nerve, so these areas were averaged together and compared between adults and fawns. For all of the retinal thickness measurements, no differences were found between fawn and adult eyes. In addition, retinal cell counts of nuclear layers were also similar between fawns and adults. In ~100 µm length of retina, the ganglion cell layer contained 8.8 ± 0.9 nuclei, the inner nuclear layer contained 55.2 ± 2.8 nuclei, and there were 8–9 rows of photoreceptor nuclei.

**Fig. 3.** Light micrograph of the retina of 0.5-year-old white-tailed deer (*Odocoileus virginianus*). The structural organization of the retina of white-tailed deer was similar to other terrestrial mammals. The layers shown include ganglion cell layer (GCL), inner plexiform layer (IPL), inner nuclear layer (INL), outer plexiform layer (OPL), outer nuclear layer (ONL), and the outer and inner segments of photoreceptors (OIP). This section was located in the superior retina where the tapetum lucidum (TL) is located. The retina was artificially detached from the retinal pigment epithelium (RPE) during processing.

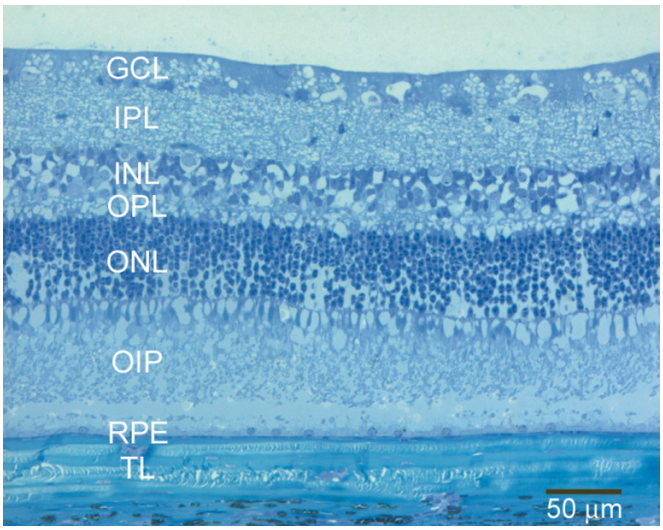


The density of cones containing M opsin was counted in three deer (0.5 years old, $n$ = 1; 3.0 years old, $n$ = 1;

**Table 2.** Retinal thickness measurements and retinal cell counts from fawn (0.5 years old; $n$ = 3) and adult (2.5–6.5 years old; $n$ = 3) white-tailed deer (*Odocoileus virginianus*) retinas.

| | Fawns | | Adults | |
|---|---|---|---|---|
| | Mean | SE | Mean | SE |
| **Retinal layer thickness (μm)** | | | | |
| Ganglion cell layer | 42.3 | 11.8 | 31.1 | 7.9 |
| Inner plexiform layer | 36.2 | 2.0 | 36.2 | 8.3 |
| Inner nuclear layer | 31.1 | 2.1 | 23.4 | 5.2 |
| Outer plexiform layer | 7.5 | 0.3 | 6.2 | 1.4 |
| Outer nuclear layer | 46.5 | 4.0 | 32.7 | 7.5 |
| Outer and inner segments | 49.4 | 4.4 | 40.8 | 11.0 |
| Total thickness | 212.9 | 20.6 | 170.4 | 40.1 |
| **Nuclei counts (per 100 μm)** | | | | |
| Ganglion cells | 9.1 | 1.0 | 8.5 | 1.2 |
| Inner nuclear layer cells | 56.0 | 3.2 | 54.0 | 3.2 |
| Rows of photoreceptors | 8.6 | 0.1 | 7.8 | 0.3 |

**Note:** The retinas were sampled from regions superior and inferior to the optic nerve.

**Table 3.** Schematic eye measurements and curvatures measured from the bisected eye in Fig. 1.

| | Mean ± SD |
|---|---|
| **Radius of curvature (mm)** | |
| Anterior lens | 8.40±0.10 |
| Posterior lens | 6.82± 0.02 |
| Anterior cornea | 8.26±0.11 |
| Posterior cornea | 7.57±0.12 |
| **Distance (mm)** | |
| Corneal thickness | 0.89±0.01 |
| Anterior chamber depth | 2.66±0.01 |
| Lens thickness | 7.87±0.01 |
| Vitreous chamber depth | 11.17±0.04 |
| **Refractive index** | |
| Cornea | 1.3771 |
| Aqueous | 1.336 |
| Lens | 1.42 |
| Vitreous | 1.336 |

**Fig. 4.** (*a*) Representative density map of medium-wavelength-antibody-labeled cones of a 0.5-year-old white-tailed deer (*Odocoileus virginianus*) labeled with JH492 antisera. The greatest density of medium-wavelength cones were located in a horizontal streak superior to the optic nerve and in the upper superior, temporal region. (*b*) Representative density map of short-wavelength-antibody-labeled cones of a 6.5-year-old white-tailed deer labeled with JH455 antisera. The density of short-wavelength cones was distributed uniformly across the entire retina.

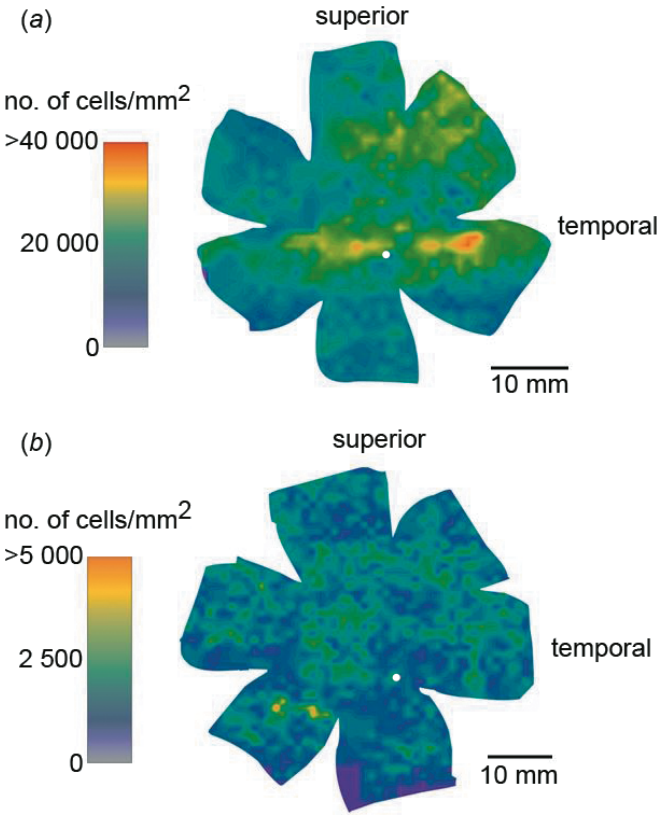


6.5 years old, $n$ = 1). The area of maximum density of M-antibody-labeled cones was characteristic of a horizontal visual streak 1–2 mm superior to the optic nerve head extending nasally and temporally. In addition, increased density of M-antibody-labeled cones was observed in the superior temporal region. The density of M-antibody-labeled cones in the retina of the 0.5-year-old female was greatest of the three deer retinas sampled and averaged 18 900/mm$^2$, ranging from a minimum of 7 500/mm$^2$ in the periphery of the inferior retina to a maximum of 42 000/mm$^2$ in the horizontal visual streak (Fig. 4*a*). The density of M-antibody-labeled cones in the retina of the 3.0-year-old female averaged 15 900/mm$^2$, ranging from a minimum of 8 400/mm$^2$ in the periphery to a maximum of 32 700/mm$^2$ in the horizontal visual streak. The density of M-antibody-labeled cones in the retina of the 6.5-year-old female averaged 16 100/mm$^2$, ranging from a minimum of 7 000/mm$^2$ to a maximum of 35 900/mm$^2$ in the horizontal visual streak.

The density of retinal cones containing S opsin was examined in two deer (1.0 year old, $n$ = 1; 6.5 years old, $n$ = 1). S-antibody-labeled cones were found at densities lower than the density of M-antibody-labeled cones with no pattern of minima or maxima across the fundus (Fig. 4*b*). The density of S-antibody-labeled cones in the retina of the 1.0-year-old female averaged 2000/mm$^2$ (range 500–4700/mm$^2$). The density of S-antibody-labeled cones in the retina of the 6.5-year-old female averaged 1400/mm$^2$ (range 500–5600/mm$^2$).

The schematic eye was constructed from the measurements shown in Table 3. The refractive error of this eye was +7.96 diopters (D). The hyperopic refraction is evident in that the rays hitting the retina are not drawn to a point focus as seen in Fig. 5*a*. The F/# was calculated to be 5.55, 2.77, 1.85, and 1.39 for pupil diameters of 3, 6, 9, and 12 mm, respectively. Figure 5*b* indicates the F/# when the eye is adjusted for emmetropia by increasing the vitreous chamber depth. The effective focal length of the eye increases when the vitreous chamber depth is adjusted to achieve emmetropia and therefore this affects the F/#, but

**Fig. 5.** (*a*) Schematic eye with a 6 mm diameter entrance pupil diameter generated by a ray tracing program for the white-tailed deer (*Odocoileus virginianus*) eye shown in Fig. 1. The eye has a hyperopic refractive error of +7.96 diopters (D), which is indicated by the parallel rays of light entering the eye creating a blur circle on the retinal surface with the focal point falling behind the retina. The measurements used to generate the eye are shown in Table 3. (*b*) A comparison of the F/# from the white-tailed deer and human schematic eyes with different entrance pupil diameters. The deer eye was calculated using a vitreous chamber depth of 11.16 or 14.47 mm to model the eye with a hyperopic refraction of +7.96 D or emmetropia (0.0 D). A maximum possible pupil diameter of 9 mm was used for the human eye and 12 mm for the deer eye. The F/# did not change significantly between different eyes for the same pupil diameters, but achieves the smallest value for the fully dilated deer eye, as would be expected for a nocturnal eye.

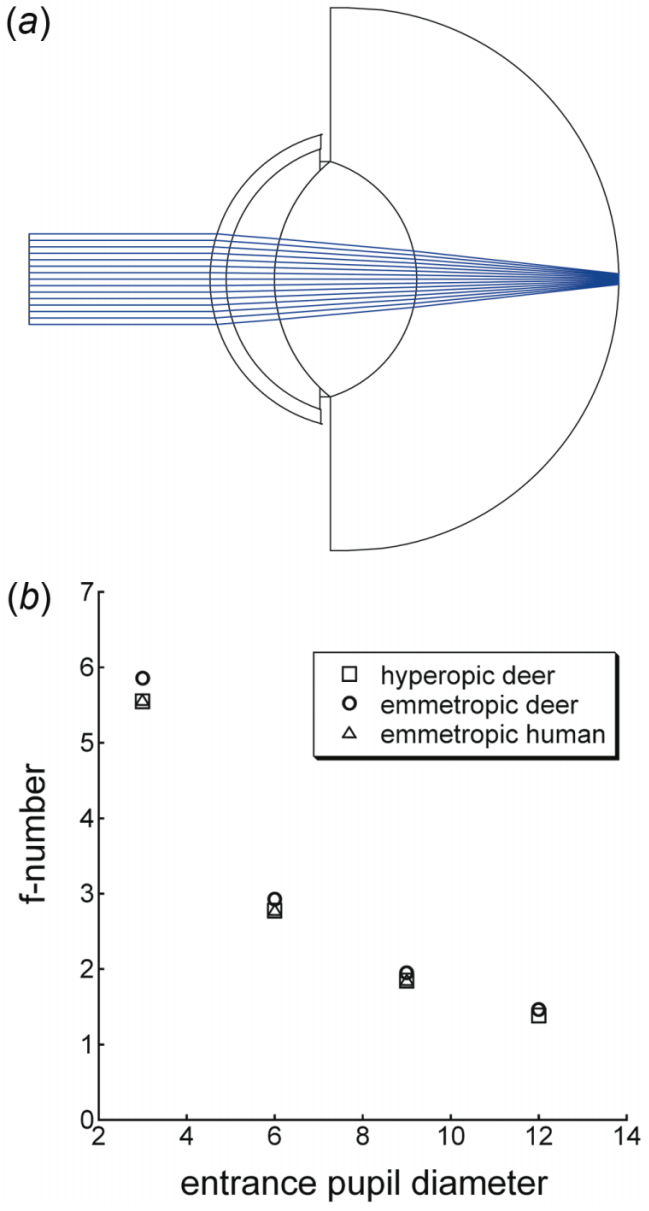


**Fig. 6.** Eye of white-tailed deer (*Odocoileus virginianus*) observed using infrared photorefraction. Multifocal ring-like structures are visible in the lens.

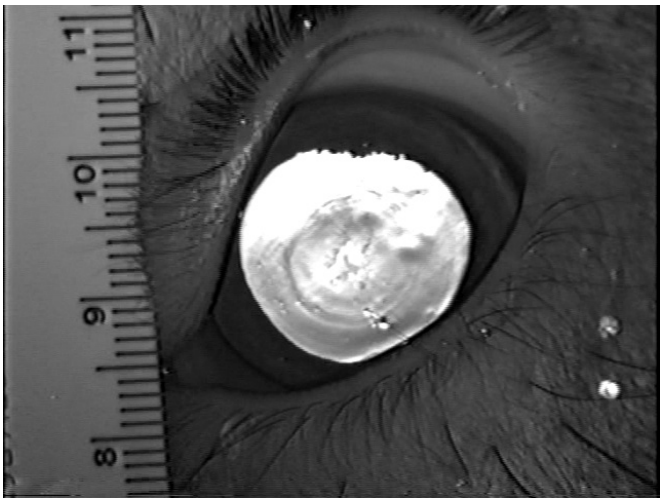


less so for the larger pupil diameters than for the smaller pupil diameters.

## Discussion

### Gross measurements

White-tailed deer have a large eye relative to their body size (~45 kg for adult females in this study) and in absolute terms compared with other species of vertebrates (Walls 1942; Ali and Klyne 1985; Howland et al. 2004). Since larger eyes have increased distance between the cornea or lens and retina and the diameter of the photoreceptor varies little among species, the large eye in the deer allows for a greater number of photoreceptors to absorb light, thus enhancing visual acuity (Walls 1942). By maximizing image size, the number of photoreceptors in the retina, and the pupil size to increase retinal illumination, larger eyes enhance visual acuity. Although illumination of the image projected on the retina decreases with increasing image size, the tapetum of deer likely compensates for such loss of brightness (see below; Ali and Klyne 1985).

The thickness of the lens is another optical feature that impacts the size of the image projected on the retina. Species with strongly nocturnal visual systems tend to have large, optically powerful lenses and large anterior chambers (e.g., mouse (*Mus musculus* L., 1758), lens thickness to axial length ratio = 0.6; M.T. Pardue, unpublished data). The large lens causes the optical center of the eye to be closer to the retina, which decreases the size of the image projected onto the retina. The projection of a smaller image increases brightness at the expense of visual acuity because fewer photoreceptors absorb light (Ali and Klyne 1985). Diurnal species, like humans, have low lens thickness to axial length ratios (lens thickness to axial length ratio = 0.2, Markowitz and Morin 1985) that projects a large image on the retina with reduced brightness, but increased acuity. The moderate lens thickness and large eye of deer (lens thickness to axial length ratio = 0.3) appears well suited for their mostly crepuscular activity patterns. Their eye likely produces an image of sufficient size and brightness for orientation

and avoidance of predators when light is at moderate levels. Similarly, nocturnal eyes tend to have large pupil diameters relative to the focal length of the eye (or short vitreous chamber depths). This equates to a small F/#, indicating increased light capture. Although deer eyes are of similar axial length and therefore focal length to that of human eyes, the deer eye has a much larger maximum pupil diameter than the human eye and therefore achieves a relatively smaller F/# for the largest pupil diameter.

The deer pupil is highly versatile to function in a range of lighting conditions. White-tailed deer possess a horizontal slit pupil. Likewise, Malmström and Kröger (2006) observed a horizontal slit pupil in other cervids, including European elk or moose (*Alces alces* (L., 1758)), red deer, and reindeer (*Rangifer tarandus* (L., 1758)). The slit pupil of white-tailed deer extends nearly the entire horizontal width of the cornea and is capable of vertical adjustment from a narrow slit in bright-light conditions dilating to a broad oval when light is limited (G.J. D'Angelo, unpublished data). The eyes in our study likely demonstrated the approximate maximum dilation of the white-tailed deer pupil since we obtained the measurements after death. The slit pupil allows species like deer with highly light-sensitive visual systems to function in full daylight without overwhelming the retina (Ali and Klyne 1985).

The horizontal slit pupil may facilitate color vision during full daylight. In a sample of terrestrial vertebrates, Malmström and Kröger (2006) found that species with slit pupils also had multifocal lenses. In a parallel study using infrared photorefraction, we observed multifocal lenses in the white-tailed deer eye (Fig. 6). Ocular media (e.g., cornea, lens, etc.) have different refractive indices for different wavelengths of light causing different wavelengths of light to focus at different distances within the eye (i.e., linear chromatic aberration; Walls 1942). Multifocal lenses have concentric zones of different refractive indices, with each zone designed to create a well-focused image on the retina for one of the spectral types of cones (Malmström and Kröger 2006). In conditions of bright light, the pupil constricts to protect the retina. When round pupils constrict, the periphery of the lens is obstructed. The slit pupil, even when constricted, enables the use of the full diameter of the lens so that all wavelengths of light may be focused on the retina (Malmström and Kröger 2006).

**Tapetum lucidum**

The tapetum lucidum consists of several layers of cells located on the outer surface of the retina, between the retinal pigment epithelium (RPE) and the choroid (Fig. 2), which enhances vision in low light. The tapetum reflects light that has already passed through the eye back to the photoreceptors a second time to increase the absorption of light and improve interpretation of visual images (Ali and Klyne 1985). Reflections from the tapetum lucidum produce the characteristic eye shine of deer and other species with light-sensitive visual systems when they are alighted by bright sources of light (Walls 1942). Like most ungulates, the tapetum of white-tailed deer is composed of regularly arranged collagen fibers (Ollivier et al. 2004).

Ollivier et al. (2004) concluded that the tapetum of herbivores was less evolved than carnivores, with tapetal variations in herbivores being more suited for maximal reflectance rather than use of specific wavelengths. However, we found that the coloration of the tapetum of white-tailed deer was of short-wavelength blues and medium-wavelength yellows, which is consistent with the spectral tuning of deer photopigments (Jacobs et al. 1994). Since scattering of light during reflection may reduce the ability of the eye to resolve the details of an image (Walls 1942), the specialized coloration of the tapetum may preserve acuity by reducing the total amount of light reflected to include only the wavelengths most perceptible to deer.

We found that the tapetum of white-tailed deer was restricted to the superior retina. Miller and Murphy (1995) suggested that a superiorly oriented tapetum in dogs (*Canis familiaris* L., 1758) functioned during both night and day. They reasoned that the superior retina receives light mostly from the ground, and the inferior retina receives light from the sky, so the tapetum probably improves the ability of animals to decipher details of the darker ground by increasing the contrast of the entire scene. In deer, tapetal function during daytime would enhance visual sensitivity and acuity, especially in dense vegetation and closed canopy forests where light infiltration is reduced and much of the visual scene is in shadow. In conditions of intense reflectivity from the ground (e.g., snow), the deer eye must adjust for tapetal function to avoid overwhelming the retina. Two such protective mechanisms are a reduction in pupil size and alteration of the sensitivity of photoreceptors in different regions of the retina (Ali and Klyne 1985).

**Retinal structure and cone density**

The structural organization of the white-tailed deer retina was similar to other vertebrates (Ali and Klyne 1985). The retinal thickness between studies is difficult to compare because of variations in tissue preparation and whether measurements included the tapetal or choroidal layers. However, adult cat retina also prepared in our laboratory had similar thickness to the deer described here (neural retina of cat without tapetum 184 ± 32 mm (Shen et al. 2006); neural retina of deer 212 ± 20.6 mm in fawns and 170.4 ± 40.1 mm in adults, Table 2).

Although our sample of deer was limited, we included a representation of ages typical of many wild populations. In this sample, retinal layer thickness and retinal nuclei counts did not differ between fawn and adult deer, although there was a trend towards thinner retina in the adult deer. These deer retinas contained 8–9 rows of photoreceptor nuclei in an area approximately in the horizontal streak. This is comparable to other species such as mice with 10–12 rows, rats with 8–9 rows, cats with 10–11 rows, and rabbits with 5–6 rows (M.T. Pardue, unpublished data). The rows of photoreceptor nuclei can vary in the human retina depending on location, with 10 rows in the fovea, 8–9 rows in the nasal retina, and only 4 rows in the temporal retina (Sharma and Ehinger 2003). However, the human fovea is adapted for diurnal vision and is composed entirely of cones (Ali and Klyne 1985).

The M cones in white-tailed deer occurred in a horizontal visual streak, similar to that described for red and roe deer (Ahnelt et al. 2006). Similar increased density of M cones, but not S cones, has also been reported for pig (Hendrickson

and Hicks 2002), cat (Linberg et al. 2001), and tammar wallaby (*Macropus eugenii* (Desmarest, 1817)) (Hemmi and Grünert 1999). The mean number of M cones in the visual streak of the white-tailed deer was ~30 000/mm$^2$. This compares with ~30 000/mm$^2$ in the red deer (Ahnelt et al. 2006), ~26 000/mm$^2$ in the roe deer (Ahnelt et al. 2006), 20 000 – 35 000/mm$^2$ in the pig (Hendrickson and Hicks 2002), over 26 000/mm$^2$ in the cat (Linberg et al. 2001), 12 000 – 18 000/mm$^2$ in the wallaby (Hemmi and Grünert 1999), and 10 364/mm$^2$ in the mouse (Williams and Jacobs 2007). In contrast, the M cone density of the human fovea centralis is >150 000/mm$^2$ (Ahnelt et al. 2006). Similar to the other non-primate mammals listed, the visual streak of white-tailed deer has far less acuity than the fovea in humans. However, the visual streak does serve to expand the field of view, without requiring any eye or head movements. Humans have close set eyes that are active, moving regularly within the orbit. Human eyes scan in conjunction across visual scenes to maximize the visual acuity of the fovea and to use binocular vision for perception of three dimensions. In contrast, deer have laterally directed eyes with limited binocular overlap (Walls 1942). As a prey species, deer must constantly monitor their surroundings to avoid predation, but also must minimize movement to avoid detection by predators. The visual streak of deer in combination with their wide-set eyes likely provides them with enhanced ability to monitor the horizon and to detect movement with a wide field of view while keeping their head stationary.

Advantages of the visual streak are not limited to motion detection by sedentary animals. Ahnelt et al. (2006) suggested that the visual streak of cheetahs (*Acinonyx jubatus* (Schreber, 1775)) was an adaptation to optimize visual sampling during chases in the savannah. The contrast of vertical habitat features against the visual streak probably aids navigation of white-tailed deer through intricate habitats when fleeing danger. Likewise, the flagging motion of their characteristic white tail across the visual streak likely helps maintain herd cohesion of deer in flight.

The visual streak and the tapetum of deer occur in the superior retina. This spatial association supports the theory that the tapetum also functions to enhance vision in daylight. Cones do not function in low-light conditions, thus the alignment of the tapetum and visual streak would be most useful when light is sufficient to stimulate function of the cones. Visual acuity and color perception of deer probably improves with increasing light intensity because the horizontal slit pupil is more constricted and concentrates the image on the central and most sensitive portion of the cone-rich visual streak. When light is limited, the reflectance of color is suppressed. Accordingly, when the pupil of deer is dilated, the rods from the entire retina may absorb light to enhance image interpretation without regard to color.

Although we found S-antibody-labeled cones at densities lower than M-antibody-labeled cones, the presence of S-anitbody-labeled cones corroborates the basis for dichromatic color vision of white-tailed deer (Jacobs et al. 1994; Calderone et al. 2003). In general, S-antibody-labeled cones were distributed evenly across the white-tailed deer retina with no distinct area of maximum density, similar to that found in other vertebrates with a visual streak (Hemmi and Grünert 1999; Linberg et al. 2001; Hendrickson and Hicks 2002). Cones sensitive to short wavelengths in deer may be a mechanism that enables their detection of predators silhouetted against the short-wavelength colors of the sky (Ahnelt et al. 2006). Such detection would be important to deer susceptible to ambushes by feline predators in trees, to bedded fawns, which are sought by ground-searching predators such as coyotes (*Canis latrans* Say, 1823) and American black bears (*Ursus americanus* Pallas, 1780), or deer in open habitats monitoring the horizon for sources of danger.

### Focal length and image brightness of white-tailed deer eye

The schematic eye calculations show the deer eye to have F/# values ranging from 5.55 to 1.39 for pupil diameters 3 to 12 mm. A human eye might have F/# values of 5.57 for a 3 mm pupil diameter and 2.78 for a 6 mm pupil diameter (Fig. 5*b*). These F/# values for the human and deer eyes are similar for the same pupil diameters. This is not surprising because the dimensions and therefore effective focal length of the deer eye is similar to that of the human eye. Retinal image brightness may therefore be comparable in human and deer eyes under photopic conditions. Certainly, under low-light conditions, the pupil diameter in the deer eye could approach 12 mm, which is far greater than the 7–8 mm maximum that might be found in a dilated human eye. Such a large pupil diameter in the deer eye would account for much smaller F/# values and consequently considerably greater retinal image brightness under scotopic conditions than attainable by a human eye.

### Conclusions

Eyes of white-tailed deer are specialized for function in a variety of habitats and lighting conditions. The visual streak of deer is similar to other cervids and provides deer with enhanced surveillance of a broad area. The tapetum lucidum improves sensitivity in low-light conditions. The spatial association of the visual streak and tapetum and the color reflectance of the tapetum likely improves the contrast of visual scenes and perception of color in daylight. The horizontal slit pupil of deer serves to protect their light-sensitive retina in bright-light conditions. In addition, the likely presence of a multifocal lens with some aberrations combined with the horizontal slit pupil would concentrate light on the visual streak to improve cone sampling under bright-light conditions. The visual system of white-tailed deer is similar to other ungulates and is well suited for sensitivity in low-light conditions and detection of predators.

## Acknowledgements

This study was funded by the Georgia Department of Transportation through the Governor's Office of Highway Safety and the National Highway Traffic Safety Administration. We acknowledge the technical support of J.G. D'Angelo, J.L. D'Angelo, J.M. D'Angelo, J.S. Falzone, A.E. Faulkner, S. Geva, and M.K. Kim. We thank G.H. Jacobs for his advice and use of laboratory facilities. J.C. Carroll, B.C. Faircloth, and R.N. Winn provided laboratory equipment. J. Nathans provided JH455 and JH492 antisera. S.B. Castleberry, A.R. De Chicchis, and M.T. Mengak provided helpful comments on the manuscript.

## References


Ahnelt, P.K., Schubert, C., Kübber-Heiss, A., Schiviz, A., and Anger, E. 2006. Independent variation of retinal S and M cone photoreceptor topographies: a survey of four families of mammals. Vis. Neurosci. **23**: 429–435. doi:10.1017/S095252380623342X. PMID:16961976.

Ali, M.A., and Klyne, M.A. 1985. Vision in vertebrates. Plenum Press, New York.

Calderone, J.B., Reese, B.E., and Jacobs, G.H. 2003. Topography of photoreceptors and retinal ganglion cells in the spotted hyena (*Crocuta crocuta*). Brain Behav. Evol. **62**: 182–192. doi:10.1159/000073270. PMID:14573992.

Geist, V. 1998. Deer of the world: their evolution, behaviour, and ecology. Stackpole Books, Mechanicsburg, Pa.

Hemmi, J.M., and Grünert, U. 1999. Distribution of photoreceptor types in the retina of a marsupial, the tammar wallaby (*Macropus eugenii*). Vis. Neurosci. **16**: 291–302. doi:10.1017/S0952523899162102. PMID:10367964.

Hendrickson, A., and Hicks, D. 2002. Distribution and density of medium- and short-wavelength selective cones in the domestic pig retina. Exp. Eye Res. **74**: 435–444. doi:10.1006/exer.2002.1181. PMID:12076087.

Howland, H.C., Merola, S., and Basarab, J.R. 2004. The allometry and scaling of the size of vertebrate eyes. Vision Res. **44**: 2043–2065. doi:10.1016/j.visres.2004.03.023. PMID:15149837.

Jacobs, G.H., Deegan, J.F., Neitz, J., Murphy, B.P., Miller, K.V., and Marchinton, R.L. 1994. Electrophysical measurements of spectral mechanisms in the retinas of two cervids: white-tailed deer (*Odocoileus virginianus*) and fallow deer (*Dama dama*). J. Comp. Physiol. A, **174**: 551–557. PMID:8006855.

Linberg, K.A., Lewis, G.P., Shaaw, C., Rex, T.S., and Fisher, S.K. 2001. Distrubtion of S- and M-comes in normal and experimentally detached cat retina. J. Comp. Neurol. **430**: 343–356. doi:10.1002/1096-9861(20010212)430:3<343::AID-CNE1035>3.0.CO;2-U. PMID:11169472.

Malmström, T., and Kröger, R.H.H. 2006. Pupil shapes and lens optics in the eyes of terrestrial vertebrates. J. Exp. Biol. **209**: 18–25. doi:10.1242/jeb.01959. PMID:16354774.

Marchinton, R.L., and Hirth, D.H. 1984. Behavior. *In* White-tailed deer ecology and management. *Edited by* L.K. Halls. Stackpole Books, Mechanicsburg, Pa. pp. 129–168.

Markowitz, S.N., and Morin, J.D. 1985. The ratio of lens thickness to axial length for biometric standardization in angle-closure glaucoma. Am. J. Ophthalmol. **99**: 400–402. PMID:3885747.

Miller, P.E., and Murphy, C.J. 1995. Vision in dogs. J. Am. Vet. Med. Assoc. **207**: 1623–1634. PMID:7493905.

Müller-Schwarze, D. 1994. The senses of deer. *In* Deer. *Edited by* D. Gerlach, S. Atwater, and J. Schnell. Stackpole Books, Mechanicsburg, Pa. pp. 58–65.

Ollivier, F.J., Samuelson, D.A., Brooks, D.E., Lewis, P.A., Kallberg, M.E., and Komáromy, A.M. 2004. Comparative morphology of the tapetum lucidum (among selected species). Vet. Ophthalmol. **7**: 11–22. doi:10.1111/j.1463-5224.2004.00318.x. PMID:14738502.

Severinghaus, C.W. 1949. Tooth development and wear as criteria of age in white-tailed deer. J. Wildl. Manage. **13**: 195–216. doi:10.2307/3796089.

Sharma, R.K., and Ehinger, B.F. 2003. Development and structure of the retina. *In* Adler's physiology of the eye, clinical application. 10th ed. *Edited by* P.L. Kaufman and A. Alm. Mosby, St. Louis, Mo. pp. 319–347.

Shen, Q., Cheng, H., Pardue, M.T., Chang, T.F., Nair, G., Vo, V.T., Shonat, R.D., and Duong, T.Q. 2006. Magnetic resonance imaging of tissue and vascular layers in the cat retina. J. Magn. Reson. Imaging, **23**: 465–472. doi:10.1002/jmri.20549. PMID:16523482.

Staknis, M.A., and Simmons, D.M. 1990. Ultrastructural evaluation of the eastern whitetail deer retina for color perception. J. Pa. Acad. Sci. **64**: 8–10.

Walls, G.L. 1942. The vertebrate eye and its adaptive radiation. Cranbrook Institute of Science, Bloomfield Hills, Mich.

Williams, G.A., and Jacobs, G.H. 2007. Cone-based vision in the aging mouse. Vision Res. **47**: 2037–2046. doi:10.1016/j.visres.2007.03.023. PMID:17509638.

Witzel, D.A., Springer, M.D., and Mollenhauer, H.H. 1978. Cone and rod photoreceptors in the white-tailed deer *Odocoileus virginianus*. Am. J. Vet. Res. **39**: 699–701. PMID:646207.